Journal of Applied Polymer Science

Uptake of Hazardous Heavy Metal Ions by Aqueous Solution of Poly(acrylamide) Prepared through Atom Transfer Radical Polymerization Process

Vivek Mishra,[1] Rajesh Kumar[2]

[1]Functional Polymer Material Laboratory, Department of Chemistry, University of Ulsan, Ulsan 680749, South Korea
[2]Organic Polymer Research Laboratory, Department of Chemistry, Centre for Advanced Studies, Faculty of Science, Banaras Hindu University, Varanasi 221005, Uttar Pradesh, India
Correspondence to: R. Kumar (E-mail: rkr_bhu@yahoo.com)

ABSTRACT: Poly(acrylamide) (PACM) used in this study was prepared through an effective atom transfer radical polymerization process and characterized by NMR, FTIR, and thermo gravimetric analysis. Resulting polymer was used for the uptake of heavy metal ions from aqueous solution. Partition coefficient, retention capacity, and metal ion uptake behavior in aqueous solution of PACM at different monomer percent conversions and effect of parameters for optimization of polymerization reaction gives thermally stable PACM. Efficiency of metal ion uptake of different molecular weights of PACM were tested in batches for Ni^{2+}, Pb^{2+}, Cu^{2+}, Zn^{2+}, and Hg^{2+} ions in single metal solution. Metal ion sorption capacities increase with increase in polymer concentration. Metal ion sorption capacities in single metal system were 6.3 mg g^{-1} Ni^{2+}, 6.0 mg g^{-1} Pb^{2+}, 6.9 mg g^{-1} Cu^{2+}, 6.2 mg g^{-1} Zn^{2+}, 22.4 mg g^{-1} Hg^{2+} for PACM of 88% conversion (Mn = 19,850). Uptake by the PACM indicates that they are effective in removing metal ions from single metal ion solutions. © 2012 Wiley Periodicals, Inc. J. Appl. Polym. Sci. 128: 3295–3307, 2013

KEYWORDS: kinetics; polyamides; radical polymerization; swelling; thermogravimetric analysis

Received 4 April 2012; accepted 26 August 2012; published online 21 September 2012
DOI: 10.1002/app.38521

INTRODUCTION

Water is necessary for the existence of life on earth. The major sources of water pollution are domestic, industrial, agricultural, solid waste, thermal, shipping water, and radioactive pollution.[1] Heavy metals released into the environment from plating plants, mining, metal finishing, welding, and alloy created a significant hazard to the public health and the environment. As we know, heavy metals are nonbiodegradable and cannot be metabolized or decayed, and they can easily enter into the food chain through a number of pathways and increase progressive toxic effects steadily in living organisms over their life period. Therefore, reliable methods are needed to remove and detect heavy metals in environmental and biological samples. The usual methods regularly used for elimination of metal ions from aqueous solution include ion-exchange,[2] solvent extraction,[3,4] chemical precipitation,[5] nanofiltration,[6] reverse osmosis,[7] and adsorption.[8–11] Adsorption process maybe one of the most popular methods for removal and has attracted significant interest because of its simplicity, handiness, and effectiveness.

Living/controlled radical polymerization has been one of the efficient techniques to synthesize well-defined polymers with low molar mass distributions and complex architectures.[12] Varieties of polymeric materials have been prepared by atom transfer radical polymerization (ATRP) method since 1995.[13–17] One of the advantages of ATRP is the control of the molecular weight and functionality. This living radical polymerization technique tolerates a wide range of functional groups in the initiator, monomer, ligand, or catalyst. A range of functionality can be introduced at an end of polymer chain using functional initiator, if the functional group remains intact during the polymerization otherwise livingness died. Furthermore, Copper-based catalyst and its complexes with nitrogen-based ligands are not only user friendly but also cost effective, which worked well for ATRP reaction[18] processes.

Poly(acrylamide) (PACM), a water-soluble polymer containing large numbers of amide side groups, has been successfully used as selective sorbents for the removal of Hg^{2+} from aqueous solution.[19–25] The amide groups on the bendable PACM chains should offer the opening for rapid interaction with aqueous Hg^{2+} to form mercury-amide linkages.[20] Nevertheless, the adsorption of Hg^{2+} onto PACM by atom transfer radical polymerization is still scarcely used. On the other hand, PACM is

Applied Polymer SCIENCE

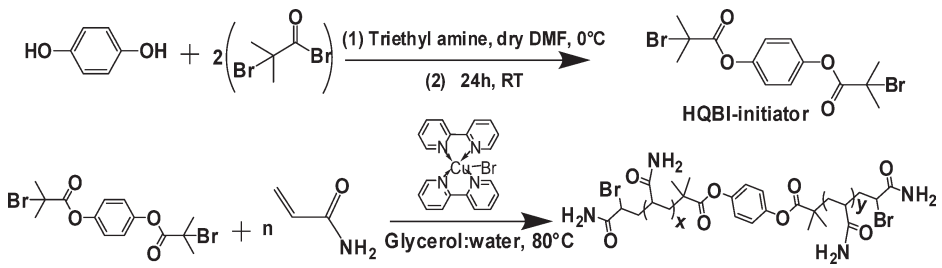

Scheme 1. Synthetic path of bifunctional initiator and polymer.

nontoxic and recently used as subdermal filler for esthetic and facial surgery.[26] PACM[27–30] is used to flocculate or coagulate solids in a liquid. It has an additional application in industries from paper manufacturing[31] and water treatment[32] through oil recovery[33] to soil modification[34] and medical applications.[35] Above and beyond these applications, it also has other multiple applications, namely, as polymer gel dosimeter for water retention owing to its high swelling capacity,[36] in electrophoresis for separation of protein and DNA samples, and as a model for drug delivery systems for studying controlled drug release profiles.[37] These potential applications of PACM were observed, when it was polymerized by conventional free radical polymerization method that gave uncontrolled molecular weight of polymer. ATRP of acrylamide (ACM) was achieved in the presence of Lewis acids, namely, $Y(OTf)_3$ or $AlCl_3$ at 130°C, which is a quite high temperature, but they got good control over the molar mass distribution.[38] In addition to this, ACM was selected to polymerize with unreported 1,4-bis(2-bromo isobutyryloxy) benzene (HQBI) as a bifunctional initiator, because bifunctional initiator is expected to polymerize at higher rate that gives higher molecular weight polymer due to the presence of two radicals per polymer chain, as we got it. If phenyl ring is present on tertiary centered carbon radical, then by resonance it is stabilizing the radical more efficiently due to that transition state energy level is reduced and product formation increases.

Thus, in this article, studies on metal ion uptake, swelling capacity, and thermal degradation of PACM synthesized under the controlled condition by ATRP process are being reported. In addition to this, synthesis of bifunctional initiator and conditions for controlled radical polymerization of ACM under ATRP process and their characterization are being reported. Study on the effect of monomer concentration, initiator concentration, catalyst/ligand ratio, and temperature on controlled radical polymerization is also being reported.

MATERIALS AND METHODS

Materials

Hydroquinone, 2,2′-bipyridyl (bpy), 2-bromo isobutyrylbromide, and triethylamine were purchased from Aldrich, Steinheim, Germany. ACM (Aldrich, Steinheim, Germany) was recrystallized twice from methanol (Merck, Mumbai, India) and dried under vacuum at room temperature. Cu(I)Br (Aldrich, Steinheim, Germany) was washed with glacial acetic acid (Merck, Mumbai, India) to remove any oxidized species, filtered, washed with ethanol (Merck, Mumbai, India), and dried under vacuum to afford a white powder. All other solvents/reagents were purchased from Merck Chemicals, Mumbai, India and used further after purification.

Preparation of 1,4-Bis(2-bromo isobutyryloxy)benzene: A Bifunctional Initiator

Hydroquinone (0.5412 g, 24.6 mmol) and triethylamine (1.38 mL, 49.2 mmol) were dissolved in 10 mL of dry dimethylformamide (DMF) under N_2 atmosphere. 2-Bromo isobutyrylbromide (1.21 mL, 49.2 mmol) was added dropwise to the solution at 0°C. After complete addition of 2-bromo isobutyrylbromide, reaction mixture was stirred at room temperature for 24 h. Completion of reaction was monitored using thin layer chromatography (TLC), when reaction was completed, triethyl ammonium bromide was removed by filtration, and the solvent was evaporated under vacuum condition. Further, the product was dissolved in 10 mL of ethyl acetate and washed with water followed by an aq. $NaHCO_3$ solution. The organic layer was separated and dried with anhydrous $MgSO_4$. After solvent removal, the product was further purified by recrystallization in petroleum ether; Yield (70%), and structure was confirmed by the spectrum of ^{1}H NMR (Figure 1) and FTIR (Figure 2).

Polymerization of ACM by 1,4-Bis(2-bromo isobutyryloxy)benzene Initiator

Glycerol–water (1 : 1, v/v), Cu(I)Br (0.0286 g, 0.2 mmol) and 2,2′-bipyridyl (0.0624 g, 0.4 mmol) were charged into 100-mL three neck Schlenk flask, and the reaction mixture was bubbled with purified N_2 gas for 30 min. Deoxygenated solution of ACM (1.420 g, 20 mmol of 1 molar solution of ACM in water) was added by syringe with stirring, and the mixture was continuously purged with N_2 gas. Polymerization was started with the addition of deoxygenated solution of 1,4-bis(2-bromo isobutyryloxy)benzene (0.0408 g, 0.1 mmol). Reaction was carried out for 24 h on oil bath, and temperature was maintained at 80°C. Two-milliliter aliquot was taken out at desired time to check the conversion by ^{1}H NMR. The deactivated complex of copper was removed from aliquot with the help of basic alumina column, and further polymer was precipitated in toluene, washed with propanol, and dried in vacuum oven at 30°C.

FTIR spectrum of PACM (KBr, cm^{-1}) (Figure 2): 3485 (ν_{N-H} asymm.stretching), 3282 (ν_{N-H} symm. broad due to absorbed moisture), 3056, 2910 (ν_{C-CH3}, Asymm. stretching vibration), 2864 (ν_{C-H} stretching vibration), 1741 (ν_{ester} carbonyl, stretching vibration), 1646 (ν_{N-CO-}, str. overlap C=O str, amide-I band), 1514 ($\nu_{C=C}$ of benzene ring, strong), 1496 (ν_{N-H} bending, amide-II band), 1411 (ν_{C-N} stretching vibration), 1349

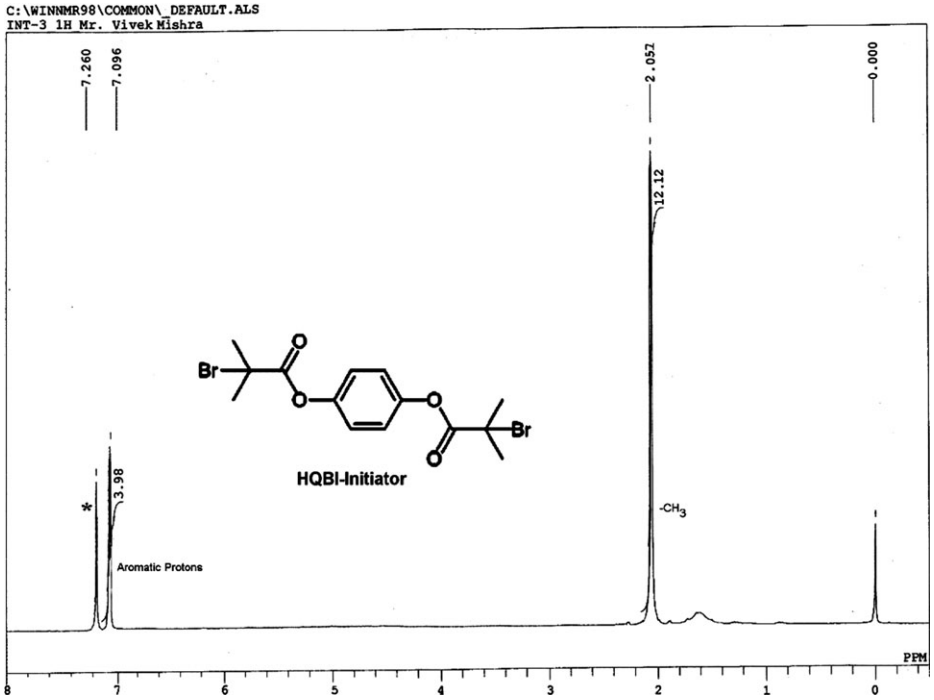

Figure 1. ^{1}H NMR spectrum of HQBI initiator

($\nu_{C—O,\ bending,\ med}$), 1256, 1198, 1121 ($\nu_{—O—C=O\text{-str.,\ or\ }}\nu_{phenol\ C—O,\ str\ broad\ strong}$), 1097 ($\nu_{C—C—C\ bending}$), 1009 ($\nu_{C—C\ str.\ of\ repeating\ unit,\ weak}$), 794, 711, 676 ($\nu_{broad\ N—H\ out\text{-}of\text{-}plane\ bending}$), 614 ($\nu_{C—Br,\ str}$), 524.

^{1}H NMR of PACM (300 MHz, deutrated dimethyl sulfoxide d_6) (Figure 3): δ 7.456–7.238 (m, br, NH_2 repeating unit), 6.806 (s, 4 H, ArH), 4.606–4.386 (t, br, —CH—Br), 2.151–2.081 ppm (d, br), 1.670–1.415 (q, br), 0.910 (s, –$4CH_3$).

NMR Analysis

The chemical structure and formation of initiator and polymer were ascertained by their ^{1}H NMR Spectra with a JEOL AL 300 FT NMR spectrometer, operating at 300 MHz resonance

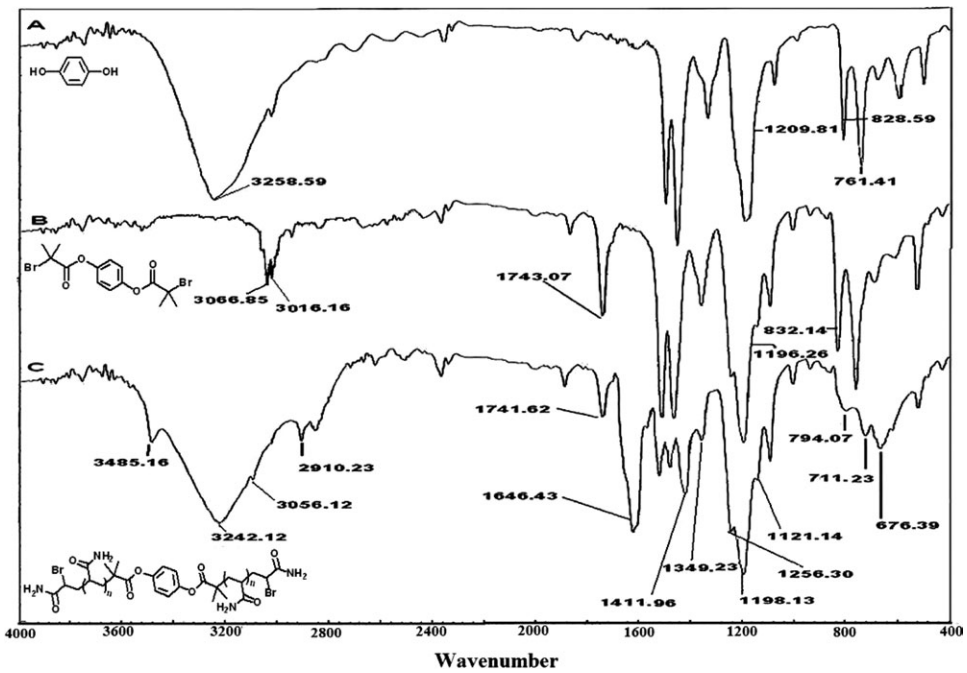

Figure 2. FTIR trace of (A) Hydroquinone, (B) 1, 4-bis (2-bromo isobutyryloxy) benzene, and (C) polymer of ACM.

Applied Polymer SCIENCE

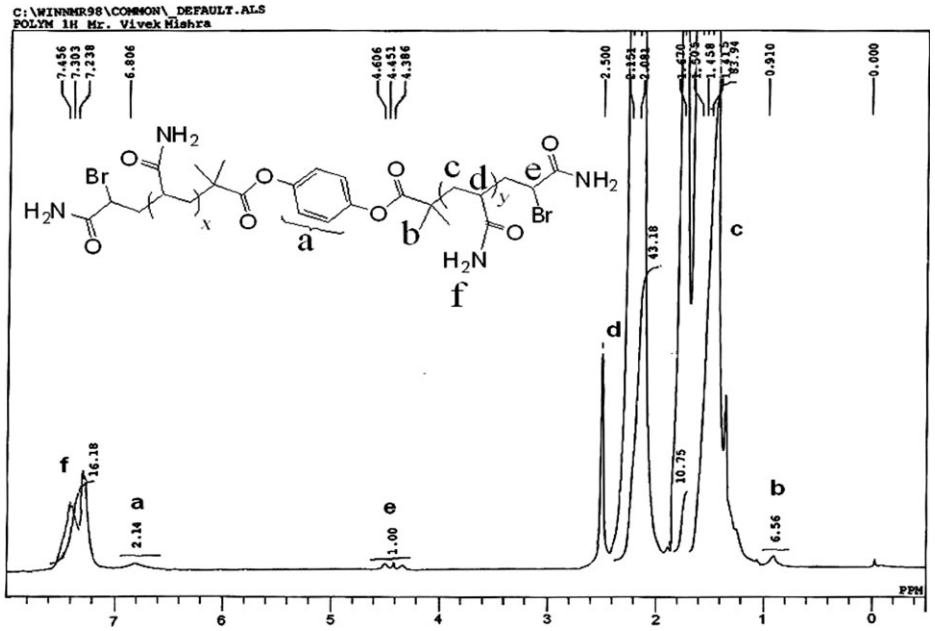

Figure 3. ^{1}H NMR spectrum of PACM initiated with 1, 4-bis (2-bromo isobutyryloxy) benzene.

frequency at 25°C using $CDCl_3$ (Figure 1) and DMSO-d_6 (Figure 3) as the solvent.

FTIR Analysis

The FTIR Spectrum of initiator and polymer (Figure 2) were determined on KBr disk with a Varian Excalibur 3000 (Palo Alto, Canada) spectrophotometer in the region 4000–400 cm^{-1}.

GPC Analysis

All the molecular weights (Mn and Mw) and molar mass distribution (Đm) of polymer samples were also determined by GPC at room temperature (ca. 30°C) using a Waters model 510 HPLC pump, a Waters series 400 differential refractometer, and three Waters Ultrahydrogel columns of 500, 250, and 120 Å pore size and 10, 6, and 6 μm bead size, respectively, which was preceded by an Ultrahydrogel guard column. An aqueous solution of 0.1 *M* $NaNO_3$ was used as eluent at a flow rate of 0.5 mL/min. The details of the preparation for GPC and filtration of these living polymers were conducted under similar conditions as reported elsewhere.[39] Poly(ethylene glycol) and poly(ethylene oxide), obtained from Waters, were used as calibration standards.

All monomer conversions for the kinetic study were estimated by ^{1}H NMR analysis with the samples directly withdrawn at desired time interval. The monomer conversion was estimated by comparing the peak areas of the protons of monomer and homopolymer. This is already mentioned in eq. (1); Mn_{NMR}, Mn_{Theo}, and initiator efficiency were calculated according to eqs. (2)–(4), respectively.

$$\%C = \frac{I_{\text{Polymer}}}{I_{\text{Polymer}} + I_{\text{Monomer}}} \times 100 \quad (1)$$

$$\text{Mn}_{\text{NMR}} = \text{Mn}_{\text{HQBI}} + \text{Mn}_{\text{ACM}} \times \text{DP}_n \quad (2)$$

where $I_{polymer}$ and $I_{monomer}$ are the integrals of the repeating unit and integral of the ACM monomer, respectively. Mn_{ACM} is

Table I. Experimental Conditions and Properties of Reactions by Normal ATRP Using HQBI as Initiator[a]

Sample	% *C*	Time (min)	$\ln[M_0/M_t]$	Mn_{theo}	Mn_{SEC}	Mn_{NMR}	Đm	Mw_{SEC}
PACM1	1	5	0.01005	550	850	740	1.52	1300
PACM2	3	15	0.03046	834	1300	1100	1.48	1900
PACM3	8	30	0.08338	1544	2370	2090	1.44	3400
PACM4	18	60	0.19845	2964	4630	4120	1.38	6400
PACM5	31	120	0.37106	4810	7400	6500	1.32	9800
PACM6	50	180	0.69315	7508	11,920	10,570	1.25	14,900
PACM7	68	360	1.13943	10,064	15,250	13,600	1.24	18,900
PACM8	81	720	1.66073	11,910	17,780	16,320	1.27	22,600
PACM9	88	1440	2.12026	12,904	19,850	17,440	1.31	26,000

[a][ACM] = 20 mmol, [Cu(I)Br] = 20 × 10^{-2} mmol, [HQBI] = 10 × 10^{-2} mmol, [bpy] = 40 × 10^{-2} mmol, Temperature = 80°C, Time = 24 h, Solvent = glycerol/water (1/1 = v/v) for ATRP process.

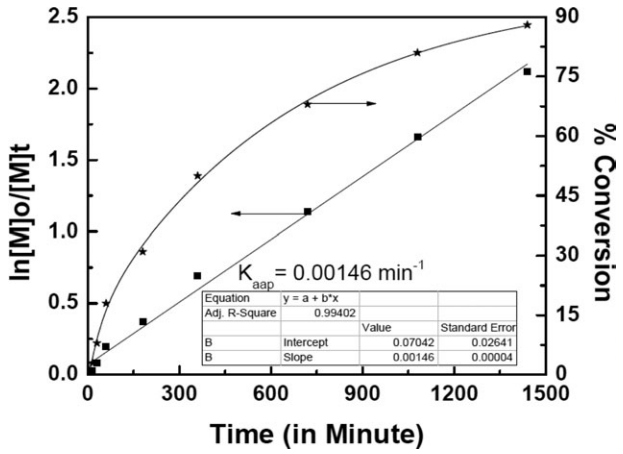

Figure 4. Plots of conversion (%) and $\ln([M]_0/[M]_t)$ versus the reaction time in glycerol/water at 80°C with an $[ACM]_0/[HQBI]_0/[Cu(I)Br]_0/[bpy]_0$ ratio of 200 : 1 : 2 : 4.

the molecular weight of ACM and Mn_{HQBI} is the molecular weight of HQBI initiator. DP_n is the degree of polymerization.

$$Mn_{Theo} = \frac{[ACM]_0}{[HQBI]_0} \times X_{ACM} \times Mn_{ACM} + Mn_{HQBI} \quad (3)$$

where $[ACM]_0$ and $[HQBI]_0$ are initial molar concentrations of ACM monomer and HQBI initiator, M_{HQBI} and M_{ACM} are molecular weight of initiator and ACM monomer, and X_{ACM} is conversion of monomer, respectively.

$$\text{Initiator efficiency, } f = Mn_{Theo}/Mn_{GPC} \quad (4)$$

Metal Ion Uptake Experiments

Stock solutions were prepared in doubled distilled water of the salts of five metal ions (Cu^{2+}, Ni^{2+}, Zn^{2+}, Pb^{2+}, and Hg^{2+}). The resulting stock solutions were stored in air tight plastic bottle. The concentrations of each metal ion were 0.5 g/L (500 ppm) in 5 mL of water. They are prepared as individual ion's solution. The metal-ion uptake studies were carried out on the different molecular weights of PACM obtained by different monomer percent conversions, that is, PACM1, 3, 5, 7, and 9 of Table I. For this, 0.05 g of different molecular weights of PACM were placed in 5 mL of solution of a metal ion of known concentration and kept for 24 h.

The strength of the unabsorbed metal ion solution and sorption behavior of the polymer was determined by a standard method,[40,41] and following parameters for metal ion uptake [Eqs. (5)–(7)] were determined:

$$\text{Percent ion uptake } (P_u) = \frac{\text{Amount of metal ion in the polymer}}{\text{Amount of metal ion in the feed}} \times 100 \quad (5)$$

$$\text{Partition coefficient } (K_d) = \frac{\text{Amount of metal ion in the polymer}}{\text{Amount of the metal ion left in the solution}} \times \frac{\text{Volume of the solution}}{\text{Weight of the dry polymer}} \quad (6)$$

$$\text{Retention capacity } (Q_r) = \frac{\text{Amount of metal ion in the polymer (mEq)}}{\text{Weight of the dry polymer}} \quad (7)$$

RESULTS AND DISCUSSION

Discussion on Synthesis of PACM

According to the mechanism of ATRP, initiator group is incorporated at α-end of the polymer chain, whereas ω-end remains a terminal halide. It can be verified by ^{1}H NMR spectrum (Figure 3). Signals at δ 6.806 and 0.910 ppm are attributed to the Ar-H and $(CH_3)_2$ groups of initiator (HQBI), respectively, incorporated in the polymer chain. Polymerization kinetics was followed *in situ* by ^{1}H NMR spectra (Figure 4 shows 88% conversion with $Mn_{[NMR]}$ = 17,440). The dependence of conversion and $\ln([M]_0/[M]_t)$, which was evaluated by the peak integration ratio of the PACM protons at δ 1.415–1.670, δ 2.081–2.150, and δ 7.238–7.456 ppm for —CH_2-group, —CH—C=O group, and —$CONH_2$ groups to vinyl peak protons at δ 7.34–7.42 (—CH) and at δ 4.38–4.49 ppm (=CH_2) of ACM monomer.

Polymerization Kinetics Studies. A semilogarithmic plot of conversion versus time gives the kinetic details of the polymerization (Figure 4). Linearity of the graph indicates the absence of termination reaction. Then, apparent rate constant can be defined by eq. (8).

$$Y = mx + c$$
$$\ln\frac{[M]_0}{[M]_t} = k_{aap}t + c \quad (8)$$

Here, k_{app} is the apparent rate constant. $\ln[M]_0/[M]_t$ is also represented as $\ln[1 - X]$. The presence of the termination and transfer reactions can be confirmed from the linearity of the plots of molecular weight and molecular weight distribution against conversion.

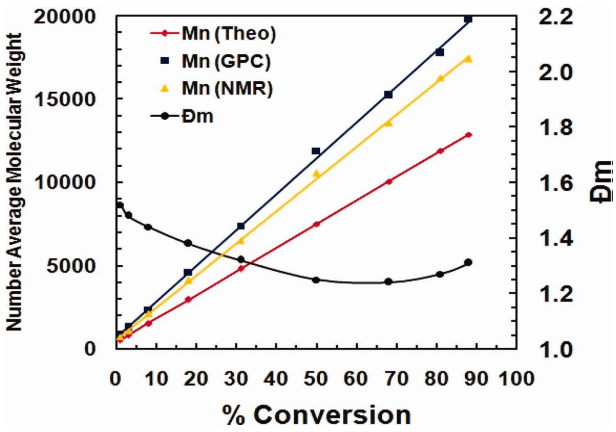

Figure 5. The relationship between the number-average molecular weight (Mn) and molar mass distribution (Đm) with conversion (%) for the polymerization of ACM in glycerol/water (1 : 1 v/v) medium at 80°C with a $[ACM]_0/[HQBI]_0/[Cu(I)Br]_0/[bpy]_0$ ratio of 200 : 1 : 1 : 2. [Color figure can be viewed in the online issue, which is available at wileyonlinelibrary.com.]

Table II. Influences of Different Reaction Parameters[a]

Run	T (°C)	[ACM] (mmol)	[ACM]/[HQBI]	[Cu(I)]/[bpy]	[ACM]/glycerol/H_2O	% C	Time (min)	$k_{aap} \times 10^{-3}$ min^{-1}	$Mn_{(theo)}$	$Mn_{(SEC)}$	DP_n	Đm
1.	80	20	200	1/2	1/1/1	88	1440	1.46	12,904	19,850	176	1.31
2.	80	30	200	1/2	1/1/1	76	1440	0.98	16,596	26,770	228	1.48
3.	80	40	200	1/2	1/1/1	64	1440	0.70	18,584	35,740	256	1.54
4.	80	20	100	1/2	1/1/1	64	1440	-	4952	8840	64	1.43
5.	80	20	050	1/2	1/1/1	51	1440	-	2219	4530	26	1.51
6.	60	20	200	1/2	1/1/1	47	1440	0.46	7082	11,800	94	1.42
7.	70	20	200	1/2	1/1/1	69	1440	0.81	10,206	16,460	138	1.42
8.	90	20	200	1/2	1/1/1	97	1440	2.35	13,188	20,600	97	1.42
9.	100	20	200	1/2	1/1/1	98	1440	2.71	14,324	20,760	98	1.36
10.	80	20	200	1/1	1/1/1	59	1440	-	8786	14,400	118	1.48
11.	80	20	200	1/3	1/1/1	91	1440	-	13,330	21,500	182	1.78
12.	80	20	200	1/2	1/0/0.5	95	900	-	13,898	25,270	190	1.74
13.	80	20	200	1/2	1/2/2	70	1440	-	10,348	17,840	140	1.46

[a][HQBI] = 10–40 × 10^{-2} mmol, [ACM] = 20–40 mmol, [Cu (I) Br] = 20 × 10^{-2} mmol., [bpy] = 20–60 × 10^{-2} mmol, solvent = glycerol : water.

The kinetic plot of polymerization at 80°C is presented in Figure 4. The linearity of the semilogarithmic plot of $\ln[M]_0/[M]_t$ versus time indicates that the polymerization is first order with respect to monomer, and the concentration of the growing radicals remains constant. Monomer conversion increases almost linearly up to 68% in 12 h.

Figure 5 shows the plot of Mn_{Theo}, Mn_{GPC}, and Mn_{NMR} versus % conversion. Mn_{Theo} values are lower than the Mn_{GPC} and Mn_{NMR} values (Figure 5 and Table I) due to the decrease in the concentration of propagating radical species with increase in conversion and/or the loss of considerable chain transfer reaction to monomer or highly reactive initiators are producing too many radicals, which are terminating at earlier stage and reducing the efficiency of initiator.[41] Although molecular weight increases linearly with increase in conversion along with the narrow molar mass distribution (Đm = 1.31–1.52). The formation of high molecular weight polymer with higher conversion can be explained by considering the higher reactivity of more stable tertiary carbon-centered radical due to the presence of phenyl group of HQBI initiator. If phenyl ring present on tertiary centered carbon radical, then by resonance it is stabilizing the radical more efficiently due to that transition state energy level is reduced, and product formation increases.

Optimization of Reaction Conditions on Polymerization

Effect of Initiator Concentration. To determine the effect of bifunctional initiator, that is, HQBI, the concentration of HQBI has been varied from 10.0 to 40 × 10^{-2} mmol (Table II, Run 1, 4, and 5) in glycerol : water (1 : 1) solvent at 80°C for 24 h. Run 1, 4, and 5 of Table II reveals that the number average molecular weight (Mn_{GPC}), conversion, and initiator efficiency decreased from 19,850 to 4530, 88% to 51%, and 0.65 to 0.49,

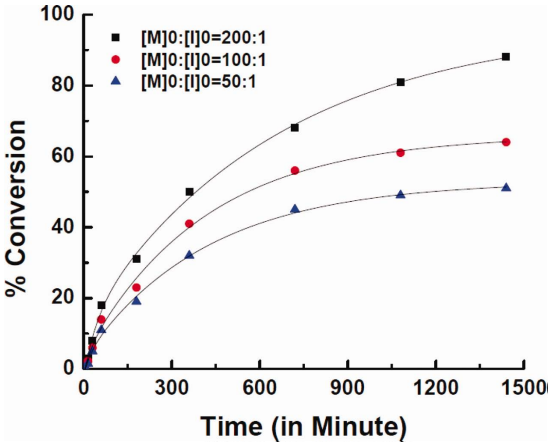

Figure 6. Effect of initiator concentration on polymerization. [Color figure can be viewed in the online issue, which is available at wileyonlinelibrary.com.]

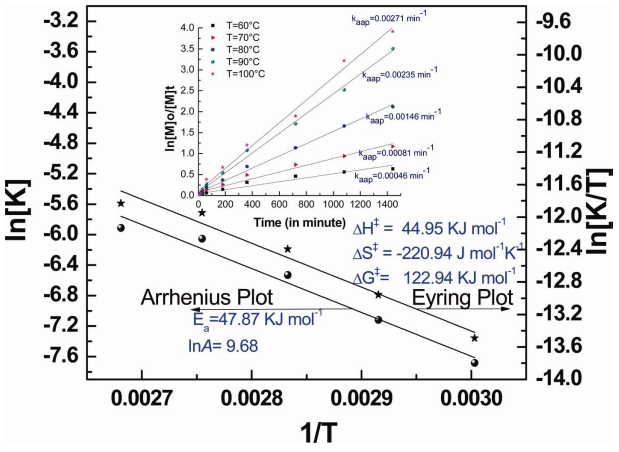

Figure 7. Effect of temperature on polymerization. [Color figure can be viewed in the online issue, which is available at wileyonlinelibrary.com.]

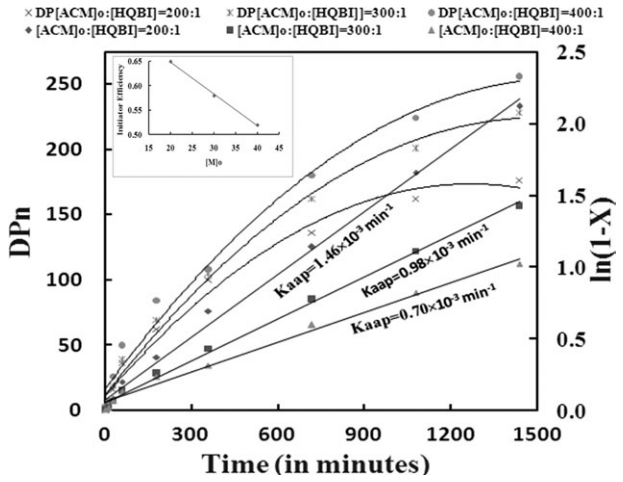

Figure 8. Effect of monomer concentration [inset] initiator efficiency with respect to $[M]_0$.

respectively, whereas molar mass distribution (Đm) increased continuously from 1.31 to 1.51. This suggests that the excess of initiator concentration shifted the ATRP equilibrium toward Cu(II) species, which in turn results more radicals, that shows the little uncontrolled polymerization of ACM (Figure 6). Run 1 of Table II, 200 : 1 ratio of ACM : HQBI shows 88% conversion in 24 h, which is a slow polymerization of ACM by HQBI initiator due to slow exchange of ligand[18,42,43] with catalyst.

Effect of Temperature and Thermodynamic Aspects. To find out the suitable temperature for living radical polymerization process, in glycerol/water mixture number of experiments were carried out at different temperatures, and 80°C was found best all variation. As shown in Run 1 and 6–9 of Table II, the conversion increases with increase in temperature. Thus, when the reaction was performed at 100°C (Run 9 of Table II), 98% conversion was observed in 24 h with 1.36 molar mass distribution. In same time at 60°C (Run 6 of Table II), 47% conversion with 1.44 molar mass distribution, at 70°C (Run 7 of Table II), 69% conversion with 1.41 molar mass distribution, at 80°C (Run 1 of Table II), 88% conversion with 1.31 molar mass distribution, and at 90°C (Run 8 of Table II), 97% conversion with 1.40 molar mass distribution were found. Therefore, polymerization at 80°C is more favorable due to good conversion with narrow molar mass distribution (Figure 7). Figure 7 also shows that the apparent rate of polymerization increases with increasing temperature because of increase of both the radical propagation rate constant and the atom transfer equilibrium constant.[44]

The temperature dependency of the apparent rate constants (k_{aap}), the magnitudes of the activation enthalpy ($\Delta H^{\ddagger}$), activation entropy ($\Delta S^{\ddagger}$), and activation energy (E_a) were determined by evaluation of the resulting straight Eyring and Arrhenius correlations (Figure 7). The negative activation entropy ($\Delta S^{\ddagger} \approx -220.94$ J mol^{-1} K^{-1}) is due to the sterically less demanding bromide moiety and greater flexibility of the activated complex. Positive values suggest that entropy increases upon achieving the transition state, which often indicates a dissociative mechanism. Negative values for $\Delta S^{\ddagger}$ indicate that entropy decreases upon achieving the transition state, which often indicates an associative mechanism. Dissociative substitution describes a pathway by which compounds interchange ligand. Due to their extremely short lifetime, transition states cannot be measured directly. They represent an energy maximum on the reaction coordinate. In bimolecular reactions, such as in an SN_2 reaction, the transition state represents one specific orientation of the reactants. That is, compared to the beginning of the reaction, the formerly infinite number of arrangements in space that the reactants might assume is reduced to only one. Thus, their entropy decreases. The entropy of activation $\Delta S^{\ddagger}$ is, therefore, negative. The higher the amount of (negative) activation entropy is, the higher the free energy of activation $\Delta G^{\ddagger} = \Delta H^{\ddagger} - T\Delta S^{\ddagger}$ is, as well. Also, in any progressive reaction, if more than one entity is present and reaction goes through transition state, in that state all entities are involved in transition state due to this entropy reduces or decreases. The negative values for $\Delta S^{\ddagger}$ suggest that at transition state movement of reactants is highly restricted, which supports the progress of reaction with time. The activation energy (E_a) (47.87 kJmol^{-1}) and activation enthalpy ($\Delta H^{\ddagger}$) (44.95 kJmol^{-1}) were not very high, suggesting the easy progress of the reaction.

Effect of Monomer Concentration. Table II (Run 1–3) and Figure 8 reveals that on varying the concentration of ACM from 20.0 to 40.0 mmol the number average molecular weight and degree of polymerization increase from 19,850 to 35,740 and 176 to 256, respectively, whereas initiator efficiency and apparent rate constant decreases continuously from 0.65 to 0.52 and 1.46×10^{-3} min^{-1} to 0.70×10^{-3} min^{-1}, respectively (Figure 8). This shows that concentration of monomer affects not only the rate of polymerization but also the initiator efficiency. This is due to the diffusion limitations experienced by radical species and/or capping agents are one of the major factors for decreasing the efficiency of radical, and the decrement in activity of catalyst is due to ligand-monomer binding in aqueous medium. In addition, it is especially true at high conversions when both

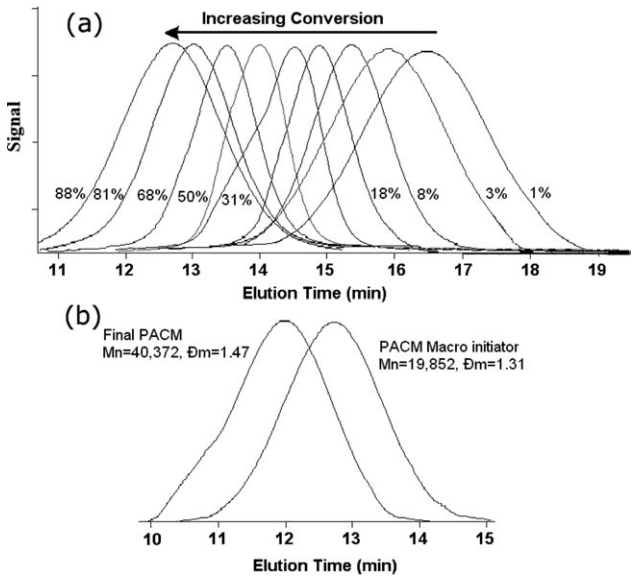

Figure 9. (a) GPC traces of HQBI_PACM polymer and (b) chain extension of PACM macroinitiator.

Table III. Absorption Studies of Metal Ions on PACM

		Percent uptake					Partition coefficient (mL g^{-1})					Retention capacity (mg.g^{-1})				
Sample	% C	Ni^{2+}	Pb^{2+}	Cu^{2+}	Zn^{2+}	Hg^{2+}	Ni^{2+}	Pb^{2+}	Cu^{2+}	Zn^{2+}	Hg^{2+}	Ni^{2+}	Pb^{2+}	Cu^{2+}	Zn^{2+}	Hg^{2+}
PACM1	1	0.8	0.4	0.8	1.0	1.9	0.8	0.4	0.8	1.1	2.0	0.4	0.2	0.4	0.5	1.0
PACM2	3	2.2	1.7	2.5	1.3	10.3	2.3	1.7	2.6	1.3	11.5	1.1	0.9	1.3	0.7	5.3
PACM3	8	5.7	4.9	5.4	4.2	18.7	6.1	5.2	5.7	4.4	23.0	2.9	2.5	2.8	2.1	9.5
PACM5	31	8.4	7.7	8.5	8.4	27.1	9.2	8.3	9.3	9.2	37.1	4.3	3.9	4.3	4.3	13.8
PACM7	68	9.5	9.1	11	9.5	35.4	10.5	10.0	12.4	10.5	54.9	4.9	4.6	5.6	4.9	18.1
PACM9	88	12.4	11.8	13.6	12.1	43.8	14.1	13.4	15.7	13.8	78.0	6.3	6.0	6.9	6.2	22.4

polymer concentration and molecular weight are high, and the system becomes viscous[45] (Run 2 and 3 of Table II). Continuous increase in degree of polymerization with increase in concentration of monomer is due to the increase in conversion of monomer into polymer. After 12 h and beyond 68% conversion, the probability of termination reaction (formation of dead polymer chains) also increases, due to that broadening of the chain length distribution occurs, which increases the molar mass distribution of the polymer (Table I, sample PACM7).

Effect of Molar Ratio of Catalyst/Ligand. The influence of concentration of ligand is investigated, and the results are shown in Table II Run 1, 10, and 11. According to Run 1, polymerization with molar ratio 1 : 2 of [Cu(I)Br] : [bpy] gives 88% conversion with 1.31 molar mass distribution. Increase in ligand concentration or decrease in CuBr concentration from 1 : 1 to 1 : 3 ratio, 59% and 91% conversion were observed along with 1.48 and 1.78 molar mass distribution, respectively. To check the optimum temperature and catalyst/ligand ratio, we used different variations and observed different Đm (polydispersity index—PDI), among them at 1 : 2 ratio for catalyst ligand, and 80°C we got minimum PDI, and optimized that condition for ATRP polymerization process. Different PDI is not significant, because the bipyridyl ligand complexes with Cu(I)Br in 2 : 1 ratio and 1 : 1 ratio or 1 : 3 ratio some Cu(I) component or bipyridyl ligand affect the polydispersity. As is well-known, in the initiation step of the ATRP, the redox reaction of CuX/ligand with the initiator would produce the radicals and Cu(II). However, bimolecular termination of polymer radicals might predominate in the initial stages before enough Cu(II) was available. Same phenomenon to the effect of temperature because if we chose lower or higher temperature instead of optimized temperature (80°C) is may be some side products.

Most important of all, the effects caused by all of these side reactions of the initiator was not proportional to the feeding amount of the initiator as expected, that is, when the most quantity of the initiator was introduced in the polymerization, these side reactions outweighed greatly its initiating reaction, which brought about the exponential influence on the molecular weight and initiator efficiency. When the initiation could not be balanced by a parallel bromine transfer reaction, it would be difficult to maintain the dynamic equilibrium between the initiation and propagation, which subsequently led to difficulty in controlling the polymerization.

Effect of Ratio of Monomer/Solvent. Three different monomer/glycerol/water solvent composition systems are studied for polymerization, and results are shown in Table II. Table II reveals that monomer/glycerol/water mixture is good composition at 1 : 1 : 1 ratio, in which the number average molecular weight of PACM are very close to their theoretical values, and this particular monomer solvent composition controls the livingness of polymerization (Table II, Run 1). This is ascribed due to the good solubility of catalyst, monomer, ligand, and initiator into the solution, which controls the viscosity of the medium. Polymerization reaction in 1 : 0 : 0.5 (monomer : glycerol : water) composition was found slightly uncontrolled up to 95% conversion with broad molar mass distribution (1.74) (Table II, Run 12). This is probably due to the low solubility of catalyst into the solution of ACM and increased viscosity of organic particles due to the formation of PACM). While with 1 : 2 : 2 (monomer : glycerol : water) composition (Table II, Run 13) shows 70% monomer conversion with moderate molar mass distribution (1.46) within 24 h. No polymerization was observed when solvent composition was changed with methanol/water due to the nontolerant nature of growing species as well as the deactivation of the catalyst in the high polar protic medium.

Chain Extension of Polymer and Their Characterization. To confirm that the polymerization is in a "living" progress, a chain extension experiment was carried out using obtained polymer as the macroinitiator using the molar ratio [Macro Initiator] : [ACM] : [Cu(I)] : [bpy] = 1(0.01 mmol ≈ 260 mg of Mn 19,850) : 200 (2 mmol) : 2 (0.02 mmol) : 4 (0.04 mmol) in 20 mL of glycerol/water mixture.

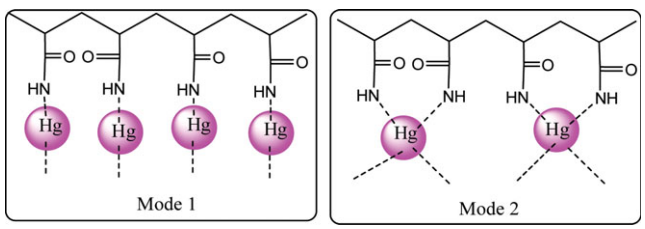

Scheme 2. Preferable mode of amide-Hg^{2+} ions interactions. [Color figure can be viewed in the online issue, which is available at wileyonlinelibrary.com.]

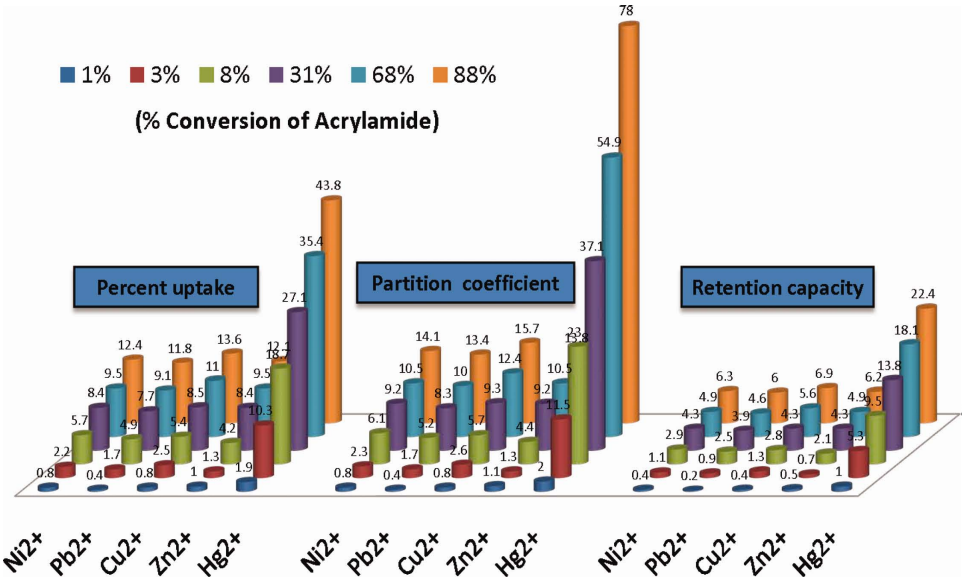

Figure 10. Partition coefficient, retention capacity, and metal ion uptake behavior in aqueous solution of PACM. [Color figure can be viewed in the online issue, which is available at wileyonlinelibrary.com.]

The plot of the monomer (%) conversion and $\ln([M]_0/[M]_t)$ versus time, the monomer (%) conversion increases almost linearly upto around 45% conversion. Therefore, the pseudofirst-order rate was followed upto 45% conversion of ACM. Molecular weight (Mn = 19,850) [Figure 9(a)] increases linearly with (%) conversion upto 45% (Mn = 40,370) [Figure 9(b)]. The observed molecular weights drifted gradually from the corresponding theoretical values with increase in conversion.

The corresponding Đm increases gradually from 1.31 to 1.47 [Figure 9(b)] with increase in (%) conversion; this broadening is due to the high viscosity of the medium. ^{1}H NMR spectrum of polymer shows the consistent growth of polymer chain as well as initiator group is incorporated at α-end of the polymer chain, whereas ω-end remains a terminal halide. This successful chain extension and characterization of polymers suggests that the polymerization process is a living progress of reaction.

Table IV. Comparison of Absorption Studies of Mercury Metal Ion on PACM through ATRP (Controlled Radical Polymerization Process) and through AIBN (Conventional Free Radical Polymerization Process)

	Percent uptake		Partition coefficient		Retention capacity	
Mw_{SEC}	ATRP	AIBN[a]	ATRP	AIBN[a]	ATRP	AIBN[a]
1300	1.9	1.2	2.0	1.6	1.0	0.6
1900	10.3	6.7	11.5	7.4	5.3	4.5
3400	18.7	10.6	23.0	18.8	9.5	7.3
6400	27.1	20.4	37.1	31.4	13.8	8.7
9800	35.4	29.5	54.9	45.2	18.1	13.4
14,900	43.8	32.7	78.0	58.9	22.4	16.6

[a]These data are based on approximate weight average molecular weight of PACM (via conventional method) not on conversion basis.

Metal ions Uptake Experiments

The results of the metal ion uptake behavior of PACM were determined in terms of the percentage ion uptake, partition coefficient, and retention capacity. The values of the percentage ion uptake for Ni^{2+} (from 0.8 to 12.4), for Pb^{2+} (from 0.4 to 11.8), for Cu^{2+} (from 0.8 to 11), for Zn^{2+} (from 1.0 to 9.5), and for Hg^{2+} (from 1.9 to 35.4) increased directly on increasing the percent conversion (Table III). Partition coefficient was increased for Ni^{2+} (from 0.8 to 14.1 mLg^{-1}), for Pb^{2+} (from 0.4 to 13.4 mLg^{-1}), for Cu^{2+} (from 0.8 to 15.7 mLg^{-1}), for Zn^{2+} (from 1.1 to 13.8 mLg^{-1}), and for Hg^{2+} (from 2.0 to 78.0 mLg^{-1}) with respect to increasing average molecular weight of polymer. And retention capacity for Ni^{2+} (from 0.4 to 6.3 mgg^{-1}), for Pb^{2+} (from 0.2 to 6.0 mgg^{-1}), for Cu^{2+} (from 0.4 to 6.9 mgg^{-1}), for Zn^{2+} (from 0.5 to 6.2 mgg^{-1}), for Hg^{2+} (from 1.0 to 22.4 mgg^{-1}) increased directly on increasing the percent conversion (Table III). These increases might be due to increase in binding sites in PACM, that is, —$CONH_2$. Table III reveals that the PACM has been shown to be an efficient for mercury metal ions. Hg^{2+} was highly absorbed in comparison to four other metal ions by the amide group, and thus it has a unique reactivity/binding toward mercuric ions, leading to the formation of amido-mercury compounds under ambient

Table V. Swelling Study at Different Temperatures

	Percent swelling (P_S) at % conversion					
Temp. (°C)	1%	3%	8%	31%	68%	88%
30	124	195	279	372	414	435
35	117	187	272	364	402	426
40	113	182	264	358	395	418
45	109	176	258	346	389	409
50	105	163	241	335	372	391

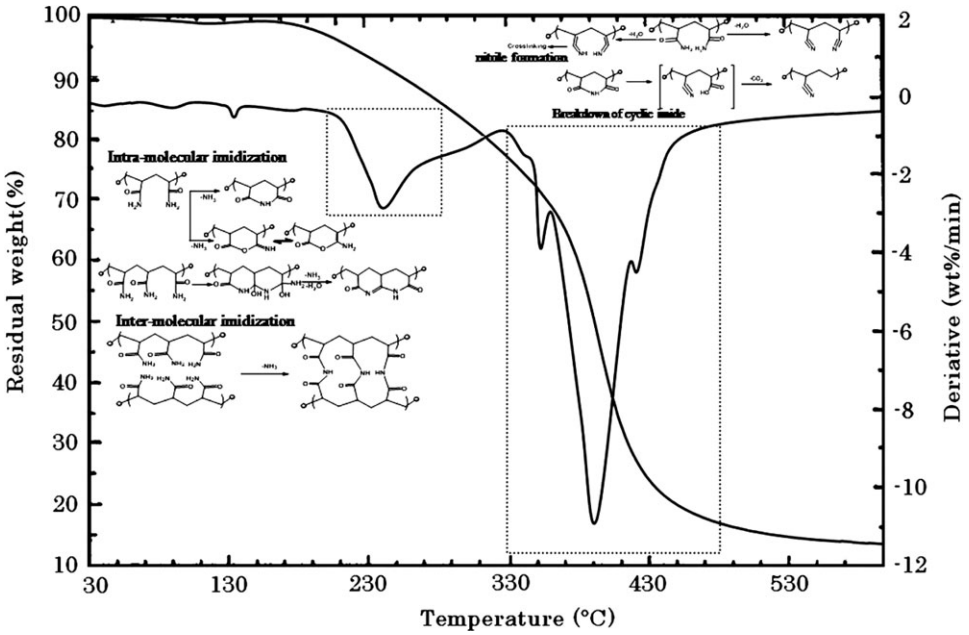

Figure 11. Thermogravimetric trace of controlled PACM.

conditions. As the electron-donating character of the amide nitrogen atom is greatly reduced by the adjacent electron-withdrawing carbonyl group, the ability of the amide groups to coordinate with other transition metal ions is extremely low. Amide compounds readily react with mercuric ions, under ordinary conditions, to give monoamido-mercury or diamido-mercury compounds. The mercury-amide linkage is believed to be strong interaction.[46] The chemistry of the mercury-amide interaction, therefore, makes the amide group unique for selective mercury removal. On the basis of this key principle and our observed results, we have verified that PACM is able to bind mercury selectively. The restoration of the loaded sorbents can be achieved by hot acetic acid without hydrolysis of amide groups (Scheme 2).

Another factor of maximum mercury binding as compare to $NiCl_2$, $CuCl_2$, $PbCl_2$, and $ZnCl_2$ is that except mercury other metals prefer only specific geometry and coordination modes. Likewise, $NiCl_2$ prefers only octahedron or square planer geometry, whereas $HgCl_2$ prefers variable of geometry. Linear geometry of $HgCl_2$ is more preferable with amide linkage, and more binding sites are available for mercury as compared to other metal ions [Scheme 2 and Figure 10]. The solubility and high binding affinity of Hg^{2+} ion may also created supportive behavior.

The metal ion uptake capability of PACM synthesized via ATRP with that synthesized using the conventional radical polymerization technique using *N, N′*-azobis(isobutylacetonitrile) (AIBN), with similar molecular weight but PDIs were compared (Table IV) and found that the well-defined PACM prepared via ATRP absorbed more metal ion due to the easily available amide sites.

The present data show improved ability of well-defined PACM in removing heavy metal ions in comparison to PACM synthesized using the conventional radical polymerization technique. This shows that ATRP synthesized PACM can be utilized for removing of Hg^{2+} from waste water in ecofriendly and nonhazardous medium.

Swelling Study

The swelling behavior of PACM was carried out in water for an hour, and the samples were prepared by taking the different (%) conversion (see Table I, Run 1–3, 5, 7, and 9) of ACM. These studies were carried out by taking 0.100 g of PACM in 20 mL of triple distilled water and kept undisturbed for 120 min at constant temperature to get the swollen equilibrium (Table V). The surface water on the swollen PACM was removed by safely pressing between the folds of the moisten filter paper, and weights were taken. Percent swelling (P_S) has been calculated using following expressions[47] [eq. (9)], and results are shown in Table V.

$$P_S = \frac{\text{Weight of swollen polymer - Weight of the dry polymer}}{\text{Weight of the dry polymer}} \times 100 \quad (9)$$

Table VI. Decomposition Temperatures of the PACM9

	Weight loss (%)								
	10	20	30	40	50	60	70	80	86
Decomposition temperature (°C)	255	315	356	378	390	400	413	450	600

Table VII. Weight Losses of PACM9 at Different Temperatures

	Decomposition temperature (°C)					
	100	200	300	400	500	600
Weight loss (%)	1	4	17	60	84	86

Table VIII. Thermo Gravimetric Analysis of the PACM9

	Sample			
	PDT (°C)	FDT (°C)	IPDT (°C)	T_{max} (°C)
PACM9	195.3	563.0	459.59	390.2

Percent swelling (P_S) of the PACM increased with increasing % *C*. This behavior could be explained on the basis of fact that ACM was hydrophilic in nature.[48] In general, for all at all conversions, swelling ratio decreases with the increase in the temperature because of the release of water owing to the gradual collapse of the PACM segment. This is because more water is absorbed in the network having lesser hydrophilicity at higher temperature. Therefore, for the change in temperature, a larger amount of water is coming out from network. Table V also reveals that percent swelling increases on increasing the % conversion of monomer at 30–50°C, which is due to the presence of more hydrophilic absorption sites (—$CONH_2$) in polymer chain at higher conversion.

Thermal Analysis

The thermal behavior of PACM was recorded on NETZSCH–Gerätebäu GmbH thermal analyzer within a temperature range 30–600°C in N_2 atmosphere at heating rate of 10°C/min. The thermal degradation of PACM is influenced by a number of factors including molecular weight, mode of synthesis, oxygen content, and the presence of impurities.[49,50] Figure 11 and Tables 6–8 show the thermogram (TG) and differential + TG for a dried sample of PACM heated at 10°C/ min from 30 to 600°C. The thermal degradation of PACM can, therefore, be divided into three regions depending on the temperature, before 200°C, the first T_{max} between 200 and 300°C and the second T_{max} between 300 and 500°C. The integral procedural decomposition

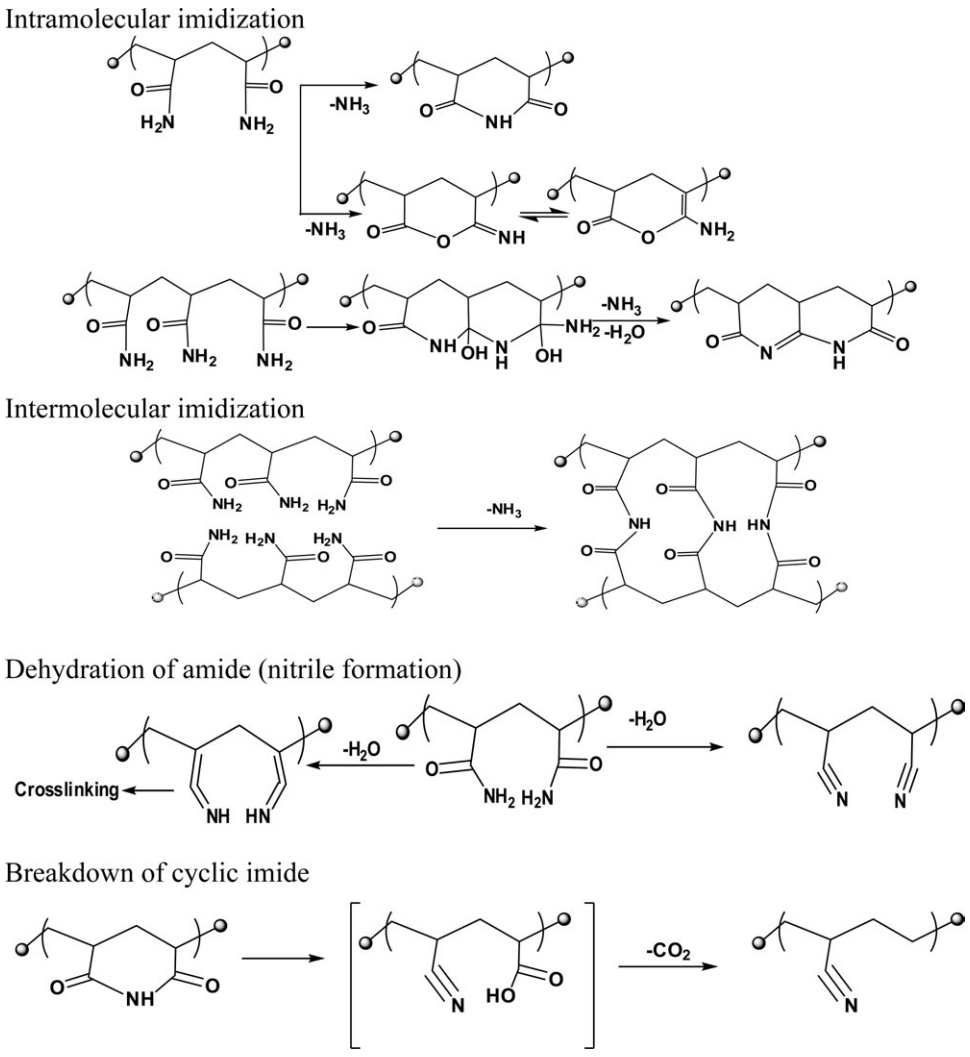

Scheme 3. Degradation pathway for PACM.

temperature (IPDT) that accounts the whole shape of the curve and it sums up all of its dips and meanderings in a single number by measuring the area under the curve. Thus, thermal stability of pure PACM has also been determined by calculating IPDT values using following equation.[51] The area under the curve divided by the total area is the total curve area, A^*, is normalized with respect to both residual mass and temperature. A^* is converted to a temperature, T_A^*, by following eq. (10).

$$T_A^* = (T_{\text{end}} - T_{\text{initial}})A^* + T_{\text{initial}} \quad (10)$$

T_A^* represents a characteristic end of volatilization temperature rather than an IPDT having practical significance. The second curve area K^* can be derived by drawing rectangle bearing X-axis upto T_A^* and the Y-axis mass fraction remaining at T_{end}. K^* is the ratio between the area under the curve (inside the rectangle) and total rectangle area. The IPDT determined by substituting A^*K^* for A^* in eq. (10).

Below 200°C, PACM is generally thermally stable and undergoes very little physical change apart from a slight mass loss. Four percent weight loss up to 200°C was observed by thermo gravimetric analysis. This weight loss is probably due to desorption of water[52] from surface and matrix-bound water of the PACM sample. There is an almost straight line from the TG curve before ~220°C corresponding to no release of volatiles. Polymer decomposition temperature (PDT) starts at 195°C and first T_{max} is observed between 200 and 300°C. At 240°C, first maximum degradation occurs with 16% of weight loss from PACM. This is due to that both intramolecular[50] and intermolecular[53] imidization reactions occur via the pendant amide groups (Scheme 2). At this stage, H_2O, NH_3, and minor quantities of CO_2 are released as byproducts of the imide formation and degradation.[54–57] A summary of the proposed thermal degradation reactions of linear PACM up to ~300°C is outlined in Scheme 3. Second T_{max} observed between 300 and 500°C. The third degradation region is initially characterized by the decomposition of imides[56,57] to form nitrile and the release of volatiles such as CO_2 and H_2O. The proposed degradation pathways for reactions above 300°C are summarized in Scheme 3. Therefore, final decomposition temperature (FDT) was found at 563°C. The Integral procedural decomposition (IPDT, 459.59°C) calculation shows the T_A^* at 469.08°C, which shows that end of volatilization of PACM. Possible thermal degradation steps are shown in Scheme 3.

CONCLUSIONS

The values of the percentage metal ion uptake, partition coefficient, and retention capacity increased directly on increasing the percent conversion. Metal ion sorption capacities in single metal system were 6.3 mgg^{-1} Ni^{2+}, 6.0 mgg^{-1} Pb^{2+}, 6.9 mgg^{-1} Cu^{2+}, 6.2 mgg^{-1} Zn^{2+}, and 22.4 mgg^{-1} Hg^{2+}, which presented PACM as an efficient mercury specific sorbent. Controlled ATRP of ACM could be achieved with lower PDI ranging from 1.31 to 1.52. Lower polymerization temperature, that is, 80°C and bifunctional sites not only committed good controllability to the ATRP of ACM but also helped to increase the polymerization rate. The synthesized PACM was equipped with bromide group at both ends, providing an easier access to further preparing the functionalized polymers by ATRP, RAFT, or click coupling. Concentration of bifunctional initiator (10 to 40 $\times$ 10^{-2} mmol) is appropriate for controlled polymerization of ACM. The activation energy (E_a), enthalpy ($\Delta H^{\ddagger}$), and entropy ($\Delta S^{\ddagger}$) were found to be 47.87 $kJmol^{-1}$, 44.95 $kJmol^{-1}$ and −220.94 J mol^{-1} K^{-1} for the present polymerization system with respect to temperature variation. Thermal analysis shows that PDT at 195°C and FDT at 563°C. Swelling ratio decreases with the increase in the temperature because of the release of water owing to the gradual collapse of the PACM segment.

ACKNOWLEDGMENTS

The authors thank the Department of Chemistry, BHU, Varanasi (India) for providing spectral and analytical facilities and Department of Science and Technology, New Delhi for financial support in the form of Fast Track Project [SR/FTP/CS-107/2005] and CSIR, New Delhi.

REFERENCES

1. Tyagi, O. D.; Mehra, M. A Text Book of Environmental Chemistry, 1st ed.; Anmol Publication Pvt. Ltd.: New Delhi, **1994, p 289.**
2. Wójtowicz, A.; Stokłosa, A. *Pol. J. Environ. Stud.* **2002,** *11*, 97.
3. Ulewicz, M.; Walkowiak, W.; Gęga, J.; Pośpiech, B. *Ars. Separatoria Acta* **2003,** *2*, 47.
4. Yun, C. H.; Prasad, R.; Guha, A. K.; Sirkar, K. K. *Ind. Eng. Chem. Res.* **1993,** *32*, 1186.
5. Taty-Costodes, V. C.; Fauduet, H.; Porte, C.; Delacroix, A. *J. Hazard. Mater.* **2003,** *105*, 121.
6. Ozaki, H.; Sharma, K.; Saktaywin, W. *Desalination* **2002,** *144*, 287.
7. Jainae, K.; Sanuwong, K.; Nuangjamnong, J.; Sukpirom, N.; Unob, F. *Chem. Eng. J.* **2010,** *160*, 586.
8. Feng, Y.; Gong, J.; Zeng, G. M.; Niu, Q. Y.; Zhang, H. Y.; Niu, C. G.; Deng, J. H.; Yan, M. *Chem. Eng. J.* **2010,** *162*, 487.
9. Peng, Q.; Liu, Y.; Zeng, G.; Xu, W.; Yang, C.; Zhang, Z. *J. Hazard. Mater.* **2010,** *177*, 676.
10. Banerjee, S. S. Chen, D. H. *J. Hazard. Mater.* **2007,** *147*, 792.
11. Mashhadizadeh, M. H.; Karami, Z. *J. Hazard. Mater.* **2011,** *190*, 1023.
12. Webster, O. W. *Science* **1991,** *251*, 887.
13. Wang, J. S.; Matyjaszewski, K. *J. Am. Chem. Soc.* **1995,** *117*, 5614.
14. Wang, J. S.; Matyjaszewski, K. *Macromolecules* **1995,** *28*, 7901.
15. Mishra, V.; Kumar, R. *Carbohydr. Polym.* **2011,** *83*, 1534.
16. Mishra, V.; Kumar, R. *Carbohydr. Polym.* **2011,** *86*, 296.
17. Mishra, V.; Kumar, R. *J. Appl. Polym. Sci.* **2012,***124*, 4475.
18. Matyjaszewski, K.; Xia, J. *Chem. Rev.* **2001,** *101*, 2921.
19. Li, N.; Bai, R. B.; Liu, C. K. *Langmuir* **2005,** *21*, 11780.

20. Sonmez, H. B.; Senkal, B. F.; Sherrington, D. C.; Bicak, N. *React. Funct. Polym.* **2003,** *55*, 1.
21. Manju, G. N.; Anoop Krishnan, K.; Vinod, V. P.; Anirudhan, T. S. *J. Hazard. Mater.* **2002,** *91*, 221.
22. Sonmez, H. B.; Senkal, B. F.; Bicak, N. *J. Polym. Sci. Part A: Polym. Chem.* **2002,** *40*, 3068.
23. Bicak, N.; Sherrington, D. C.; Senkal, B. F. *React. Funct. Polym.* **1999,** *41*, 69.
24. Shibi, I. G.; Anirudhan, T. S. *Ind. Eng. Chem. Res.* **2002,** *41*, 5341.
25. Liu, P.; Guo, J. S. *Colloids Surf. A: Physicochem. Eng. Aspects* **2006, 282/283, 498.**
26. Breiting, V.; Aasted, A.; Jørgensen, A.; Opitz, P.; Rosetzsky, A. *Aesthetic Plast. Surg.* **2004,** *28*, 45.
27. Srivastava, A.; Mishra, V.; Singh, S. K.; Kumar, R. *e-Polymers* **2009,** *006*, 1.
28. Srivastava, A.; Mishra, V.; Singh, S. K.; Kumar, R. *J. Appl. Polym. Sci.* **2010,** *115*, 2375.
29. Srivastava, A.; Mishra, V.; Singh, P.; Srivastava, A.; Kumar, R. *J. Therm. Anal. Calorim.* **2012,** *107*, 211.
30. Mishra, V.; Kumar, R. *Trends Carbohydr. Res.* **2012**, *4*, 1.
31. Reynolds, W. J.; Wasser, R. B. In Pulp and Paper Chemistry and Chemical Technology; Casey, J. P.Ed.; Wiley-Interscience: New York, **1981; Vol. 3.**
32. Flock, H. G.; Rausch, E. G. In Water Soluble Polymers; Bikales, N. M., Ed.; Plenum Press: New York, **1973.**
33. Chang, H. L. *J. Pet Technol.* **1978,** *30*, 1113.
34. Roth, R.W. U. S. Pat. 2,801,985 (**1957**).
35. Hoffman, S. *J. Controlled Release* **1987,** *4*, 213.
36. Fuxman, A. M.; McAuley, K. B.; Schreiner, L. *J. Chem. Eng. Sci.* **2005,** *60*, 1277.
37. Cohen, Y.; Ramon, O.; Kopelman, I. J.; Mizrahi, S. *J. Polym. Sci. Part B: Polym. Phys.* **1992,** *30*, 1055.
38. Patten, T. E.; Matyjaszewski, K. *Acc. Chem. Res.* **1999,** *32*, 895.
39. Jewrajka, S. K.; Mandal, B. M. *Macromolecules* **2003,** *36*, 311.
40. Basset, J.; Denny, R. C.; Jeffery, G. H.; Mendham, J. Vogel's Text Book of Quantitative Analysis, 4th ed.; William Clowes and Sons: London **1978; p 324.**
41. Rivas, B. L.; Maturana, H. A.; Molina, M. J.; Gomez-Anton, M. R.; Pierola, I. F. *J. Appl. Polym. Sci.* **1998,** *67*, 1109.
42. Xiao, D.; Wirth, M. *J. Macromolecules* **2002,** *35*, 2919.
43. Mantovani, G.; Lecolley, F.; Tao, L.; Haddleton, D. M.; Clerx, J.; Cornelissen, J. J. L. M.; Velonia, K. *J. Am. Chem. Soc.* **2005,** *127*, 2966.
44. Sha, K.; Li, D.; Li, Y.; Ai, P.; Wang, W.; Xu, Y.; Liu, X.; Wu, M.; Wang, S.; Zhang, B.; Wang, J. *Polymer* **2006,** *47*, 4292.
45. Destarac, M.; Boutevin, B.; Matyjaszewski, K. *ACS Symp. Ser.* **2000,** *768*, 234.
46. Ley, H.; Kissel, H. *Chem. Ber.* **1899,** *32*, 1358.
47. Sharma, B. J.; Kumar, V.; Soni, P. L. *Trends Carbohydr. Chem.* **1999,** *5*, 5.
48. Pourjavadi, A.; Mahdavinia, G. R. *Turk. J. Chem.* **2006,** *5*, 30595.
49. Tolstikh, L. I.; Akimov, N. I.; Golubeva, I. A.; Shvetsov, I. A. *Int. J. Polym. Mater.* **1992,** *17*, 177.
50. Leung, W. M.; Axelson, D. E.; Van Dyke, J. D. *J. Polym. Sci. Part A: Polym. Chem.* **1987, 25, 1825.**
51. Doyle, C. D. *Anal. Chem.* **1961,** *33*, 77.
52. Silva, M. E. S. R. E.; Dutra, E. R.; Mano, V.; Machado, J. C. *Polym. Degrad. Stab.* **2000,** *67*, 491.
53. Vilcu, R.; Irinei, F.; Ionescu-Bujor, J.; Olteanu, M.; Demetrescu, I. *J. Therm. Anal.* **1985,** *30*, 495.
54. Van Dyke, J. D.; Kasperski, K. L. *J. Polym. Sci. Part A: Polym. Chem.* **1993, 31, 1807.**
55. Maurer, J. J.; Harvey, G. D. *Thermochim. Acta* **1987,** *121*, 295.
56. Toth, I.; Szepvolgyi, J.; Jakab, E.; Szabo, P.; Szekely, T. *Thermochim. Acta* **1990,** *170*, 155.
57. Vilcu, R.; Bujor, I. I.; Olteanu, O.; Demetrescu, I. *J. Appl. Polym. Sci.* **1987,** *33*, 2431.